J Mater Sci: Mater Med (2009) 20:351–358
DOI 10.1007/s10856-008-3591-2

Fabrication and biological characteristics of β-tricalcium phosphate porous ceramic scaffolds reinforced with calcium phosphate glass

S. Cai · G. H. Xu · X. Z. Yu · W. J. Zhang · Z. Y. Xiao · K. D. Yao

Received: 26 September 2007 / Accepted: 4 September 2008 / Published online: 21 September 2008

Abstract The fabrication process, compressive strength and biocompatibility of porous β-tricalcium phosphate (β-TCP) ceramic scaffolds reinforced with $45P_2O_5$–$22CaO$–$25Na_2O$–$8MgO$ bioglass (β-TCP/BG) were investigated for their suitability as bone engineering materials. Porous β-TCP/BG scaffolds with macropore sizes of 200–500 μm were prepared by coating porous polyurethane template with β-TCP/BG slurry. The β-TCP/BG scaffolds showed interconnected porous structures and exhibited enhanced mechanical properties to those pure β-TCP scaffolds. In order to assess the effects of chemical composition of this bioglass on the behavior of osteoblasts cultured in vitro, porous scaffolds were immersed in simulated body fluid (SBF) for 2 weeks, and original specimens (without soaked in SBF) seeded with MC3T3-E1 were cultured for the same period. The ability of inducing apatite crystals in simulated body fluid and the attachment of osteoblasts were examined. Results suggest that apatite agglomerates are formed on the surface of the β-TCP/BG scaffolds and its Ca/P molar ratio is ~1.42. Controlling the crystallization from the β-TCP/BG matrix could influence the releasing speed of inorganic ions and further adjust the microenvironment of the solution around the β-TCP/BG, which could improve the interaction between osteoblasts and the scaffolds.

S. Cai · X. Z. Yu · W. J. Zhang · Z. Y. Xiao
Key Laboratory for Advanced Ceramics and Machining Technology of Ministry of Education, Tianjin University, Tianjin 300072, People's Republic of China

G. H. Xu (✉)
Shanghai Changzheng Hospital, Shanghai 200003, People's Republic of China
e-mail: guohuaxumail@yahoo.com.cn

K. D. Yao
Research Institute of Polymeric Materials, Tianjin 300072, People's Republic of China

1 Introduction

Bone tissue engineering presents an alternative approach to the repair and regeneration of damaged human tissue, avoiding the need for a permanent implant [1]. To guide in vitro or vivo tissue regeneration, it is necessary to obtain appropriate scaffold materials, which satisfy all the requirements, such as biocompatible, osteoconductivity, controlled degradation, mechanical properties, formability, etc. In addition to these mentioned requirements, scaffolds for bone tissue engineering must also have a high interconnected macro porosity to promote cell attachment, proliferation and provides pathways for biofluids [2, 3]. However, a material generally weakens as its porosity increases. Among the possible candidate materials for bone tissue engineering scaffold, tricalcium phosphate (TCP), especially β-TCP ceramic, is known to be biocompatible, osteoconductive and with a high biodegradation rate. However, it does not have the desired mechanical properties such as bending strength and fracture toughness. The most common approaches of improving the mechanical properties were the incorporation of reinforcing phases, in the form of particles, platelets and whiskers, of different ceramic oxides or/and metal dispersions [4–8]. Among them, although zirconia (ZrO_2) has been found to retain high mechanical strength and toughness without degrading the biocompatibility of the matrix when it is incorporated as a second phase [9–12], our research showed that the presence of ZrO_2 grains reduced the ability to form a chemical bond directly with natural bone. Bioglass

strengthening calcium phosphate ceramics is also an available way to improve the matrix's mechanical properties. It is confirmed that HA matrix composites reinforced with bioglass exhibit greater biological activities than commercial HA [13–15]. The presence of bioactive glassy phase can provide fast response in terms of bone healing and bonding processes. Most of the bioglasses for strengthening calcium phosphate ceramics are silicate glasses [16]. Compared with silicate glasses, silicon-free calcium phosphate glasses have the advantages of being close to the composition of natural bone. Nagase et al. [17] showed that calcium phosphate glass ($50CaO–50P_2O_5$ in mol%) doesn't show toxicity from in vivo experiments. It is difficult, however, to prepare calcium phosphate glasses with composition of high CaO/P_2O_5 ratio (e. g., ≥ 1) for implantation application. Although several calcium phosphate glasses with high CaO/P_2O_5 ratio have been developed by introducing small amount of Na_2O, TiO_2, MgO, et al., no calcium phosphate was formed newly on the glass-ceramics derived from $60CaO \cdot 30P_2O_5 \cdot 7Na_2O \cdot 3MgO$ by soaking in SBF at 37°C [18]. It implied that this glass didn't show bioactivity. It was considered that Ca^{2+} content directly influence the bioactivity, because too much dissolved Ca^{2+}, PO_4^{3-}, leading to sharp change of the microenvironment, may disturbed the activity of host cells and create adverse effects on tissue [19]. Compared with calcium phosphate glass with high CaO/P_2O_5 ratio (e. g., ≥ 1), low CaO/P_2O_5 ratio glass is easy to obtain and more soluble. However, in vitro studies have shown that too high a solubility is detrimental to cell activity [20]. In order to control the solubility, some researcher studied the effect of doping these glasses with various ions. The addition of iron phosphate increased the cross-linkage that makes the glass structure less susceptible to water attack. Hence, there is a great potential for these glasses to be used for degradable temporary scaffolds for the regeneration of hard and soft tissues. Previous work has also shown that these glasses with a fixed P_2O_5 content of 45 mol% by doping with various ions gives a good range of glasses, which melt and cast easily and show good biocompatibility in vitro [21].

In order to control the solubility of bioglass and improve the strength and biocompatability of β-TCP porous ceramic, a glass composition based on the P_2O_5–CaO–Na_2O–MgO system has been prepared in the present work. Thermal properties were determined to guide the choice of parameters for heat-treatment and sintering scheme of the glass reinforcing β-TCP porous ceramic scaffolds, which were fabricated by a polyurethane sponged technique. The influence of the glass on sintering behavior, compressive strength, and the effects of the controlled crystallization from glass matrix on the bioactivity of porous scaffolds were investigated.

2 Materials and methods

2.1 Materials and processing

The composition of the $CaO–P_2O_5$ based glass in molar percentage is $45P_2O_5–22CaO–25Na_2O–8MgO$. The starting materials, which were analytical regent grade $CaCO_3$, Na_2CO_3, $(MgCO_3)_4\,Mg(OH)_2 \cdot 5H_2O$ and $NH_4H_2PO_4$, were weighed and placed with distilled water in a pyrex beaker and stirred to make a homogeneous slurry. The slurry was dried at about 100°C and the resulting powder was melted in a platinum crucible at 1,100°C for 4 h, followed by quenching in air to room temperature. The quenched powder was crushed into the fine powder and sized by 100-mesh and stored in a dry cabinet. The glass powder was analysed by differential thermal analysis (DSC) through equipment (NETZSCH STA499C) with a heating rate of 5°C/min to determine the glass transition temperature, crystallization and the melting range. The obtained DSC result was chosen as guiding parameters for heat-treatment scheme for the crystalline precipitation from the ceramic-glass matrix during the followed sintering. An α-Al_2O_3 crucible was used as reference and the glass was heated in a platinum crucible from room temperature to 1,200°C at a uniform heating rate of 10°C/min.

β-TCP powder was synthesized by mechanochemical method using $CaHPO_4 \cdot 2H_2O$ and $CaCO_3$. The processing details are described elsewhere [22].

2.2 Porous scaffolds

To prepare porous green samples, a mixture with weight ratio of 80:20 of β-TCP to glass powder was prepared by ball mixing for 4 h at a speed of 600 rpm in distilled water with zirconia ball. 0.6 wt% PVA aqueous solution that acts as binder was poured into the mixture while stirring to obtain a well-dispersed slurry. Gelatin shows reversible swelling change in response to temperature. At a temperature of about 40°C, gelatin aqueous solution is in the sol state and forms physical thermoreversible gels on cooling [23, 24]. In order to get an interconnected microporous structure in the sintered scaffolds, the swelling gelatin granules were used as micropore formers in this present work. 1 wt% gelatin particles (purchased from Qing Dao University, CHINA) were weighed in air-dried conditions and then added to above slurry which kept at temperature of 40°C. The polyurethane sponge (45ppi, purchased from Da Di company, CHINA) were immersed in the slurry and compressed to squeeze the excess slurry out. Then the impregnated foams were aged in air with 80% humidity at least 24 h. To remove the polyurethane foams and get the desired dried porous scaffolds, the impregnated foams were sintered in an auto-controlled stove at 1,100°C for 2 h

using the heating scheme described as following: specimens were heated at a rate of 1.5°C/min from room temperature to 150°C; from 150°C to 380°C, at a rate of 0.5°C/min and held at this temperature for 1 h; from 380°C to 600°C, at 1°C/min; from 600°C to 1,100°C, at 2.5°C/min and held for 2 h; heat treatment performed at 712°C and 778°C for 3 h respectively. Then the specimens were cooled down in the furnace.

2.3 Characterization of porous scaffolds

The porosity of the β-TCP/BG scaffolds was determined by mercury porosimetry (Autopore II, 9220). Four specimens were selected to determine porosity with an error of less than 1% of the measured porosity value.

Identification of the crystalline phases of the bioglass powders, dried slurry and β-TCP/BG samples was carried out by X-ray diffraction analysis (D/MAX-2500). The diffraction patterns were collected with Ca Kα radiation over an angular range of 10–60°(2θ values). Microstructural observations of the porous structures were determined by environmental scanning electron microscope (ESEM, XL30).

The compressive strength was evaluated by INSTRON universal testing machine with a crosshead speed of 1 mm/min. Every reported data is the average of at least 5 specimens ($\Phi = 6$ mm, height $= 10$ mm).

The concentration of ions from β-TCP/BG and β-TCP samples that dissolved in distilled water (pH $= 6.9$) was examined by plasma atomic emission spectroscope (ICP-ARL3580).

2.4 In vitro experiment

β-TCP/BG and pure β-TCP porous scaffolds were placed into the simulated body fluid (SBF) which is an aqueous solution consisting of Ca^{2+}, 2.5 mM; Na^{+}, 142.0 mM; Mg^{2+}, 1.5 mM: K^{+}, 5.0 mM; Cl^{-}, 148.3 mM; HCO_3^{-}, 4.2 mM; HPO_4^{2-}, 1.0 mM; SO_4^{2-}, 0.5 mM; $(CH_2OH)_3CNH_2$, 50 mM and 45.0 mM HCl at pH 7.4 at 37°C for different days. Eight specimens of each β-TCP/BG and pure β-TCP porous scaffolds were used for the SBF immersion. After immersion, the specimens were removed from the SBF and washed gently with distilled water and then dried at room temperature for the use of the SEM observation. The microstructure and Ca/P molar ratio of deposited phases were examined by ESEM (equipped with EDS, XL30).

2.5 Cell culture on porous scaffolds

The MC3T3-E1 cells, after digested by 0.25% trypsin, were made into a kind of suspension, which density was about 1×10^6cells/ml. 1 ml of cell suspension was inoculated into the porous β-TCP and β-TCP/BG matrices (sizes: $5 \times 5 \times 15$ mm) respectively under the pressure. Then, the scaffolds compounded with MC3T3-E1 cells were to cultivate in the culture cabinet with the condition of 37°C, 5%CO_2 and saturated humidity. After 2 h, they were taken out and placed in 35 mm $\times$ 10 mm culture capsules, and 4–5 ml Dulbecco's Modified Eagle Medium (DMEM, Gibco) containing 10% fetal bovine serum was added. They were further incubated in the culture capsules with the condition of 37°C, 5%CO_2 and saturated humidity. The culture media were changed every 3 days.

After 2 weeks of co-cultivation with cells, scaffold materials were washed with phosphate buffered saline liquid (PBS). Cells were fixed with 2% glutaraldehyde for 2 h, and then washed again by PBS liquid for 20 minutes after drawn off the fixed agent. They were fixed for 1 h in osmic acid, washed again by PBS liquid, and then dehydrated through graded alcohol solution, displaced by acetic acid iso-valeraldehyde, dried in the critical point. The growth and secretion of MC3T3-E1 cells on the porosity surface of the scaffolds were observed by scanning electron microscopy (ESEM, XL30).

The MC3T3-E1 cells were seeded into 24 pieces of porous β-TCP and β-TCP/BG scaffold (sizes: $5 \times 5 \times 15$ mm) respectively and allowed to proliferate under culture conditions, 8 pieces scaffold respectively were dislodged and the number of cells were evaluated during 2 days, 4 days and 6 days after cultured. After blowing the collected cell suspension well-distributed, drawing a little to the blood cell counting chamber, then taking count of the cells in the whole four big panels of the counting chamber under microscope. The cell population per milliliter can be described by the above counted value divided by four and then multiplied by the fourth power of ten, and repeating this process for three times. Note that the cell suspension should be blown over again before each counting process, thereby preventing the cells from deposited.

3 Results and discussion

3.1 Characteristics of porous scaffolds

As shown in Fig. 1b, the XRD results for quenched glass powder after heat treatment at temperatures of 712°C and 778°C reveal the presence of $Na_4P_2O_7$ (JCPDS 10-0187), $Ca_9MgNa(PO_4)_7$ (JCPDS 45-0136) and a little residual amorphous glass. When the well-dispersed slurry was dried, five crystallization phases can be observed from Fig. 1c. As compared to Fig. 1b, three new crystal phases, namely Na_3PO_4 (JCPDS 31-1318), Na_2HPO_4 (JCPDS

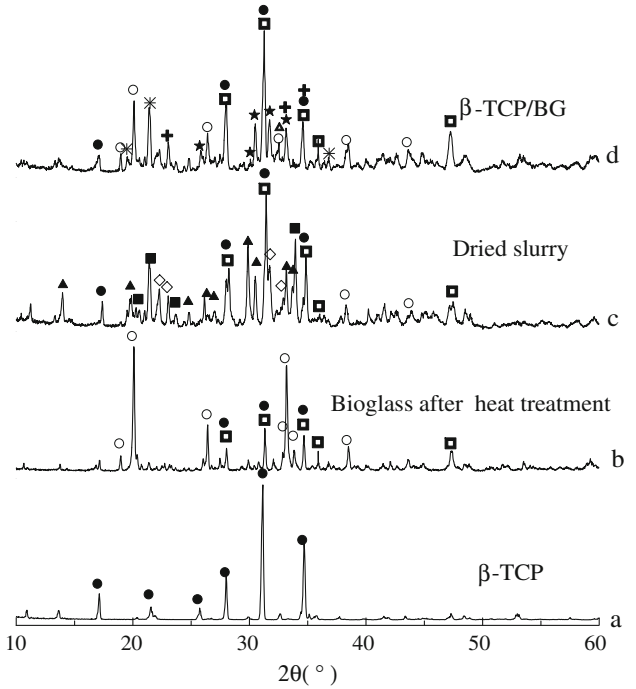

Fig. 1 XRD patterns of β-TCP powder (a), heat-treated bioglass powder (b) and the sintered ceramic-glass sample (c): ●: β-TCP, ◯: $Na_4P_2O_7$, ◘: $Ca_9MgNa(PO_4)_7$, ◇: Na_2HPO_4, ■: Na_3PO_4, ▲: $Na_4HP_3O_{10} \cdot H_2O$, + $NaCaPO_4$, ★: $Ca_4O(PO_4)_2$, ✳: unknown phase

35-0735) and $Na_4HP_3O_{10} \cdot H_2O$ (JCPDS 15-0513) are detected and $Na_4P_2O_7$ is not found in the slurry sample, which means that $Na_4P_2O_7$ is excluded by some reactions in the water medium during the preparation of the slurry. As the β-TCP/BG specimens are sintered at 1,100°C, the XRD pattern in Fig. 1d shows that all the new phases formed during the preparing of the slurry disappear and $Na_4P_2O_7$ can be observed again, but the intensity decreases as compared to Fig. 1b. Besides β-TCP and $Ca_9MgNa(PO_4)_7$, new phases $NaCaPO_4$ (JCPDS 29-1193), $Ca_4O(PO_4)_2$ (JCPDS 25-1137) and unknown phase can be detected, suggesting that some reactions occurred during sintering process and produced above new phases. The appearance of $Na_4P_2O_7$ is associated with the directly decomposition of Na_2HPO_4 and $Na_4HP_3O_{10} \cdot H_2O$ at high temperature. $Ca_4O(PO_4)_2$ and $NaCaPO_4$ are the results of the complex reactions of residual glass, β-TCP and Na_3PO_4 during sintering. Ando and Matsuno [25] have investigated the $Ca_3(PO4)_2$–$CaNaPO_4$ system and claimed that at high temperatures (650–980°C) $CaNaPO_4$ dissolves large amounts of $Ca_3(PO_4)_2$ to form an α-rhenanite solid solution. The unknown phase may be related with the solid solution. However, the intensity of β-TCP in Fig. 1d keeps almost the same as that in Fig. 1c even if the sintering temperature is 1,100°C. So further and detail research should be done before giving a conclusion.

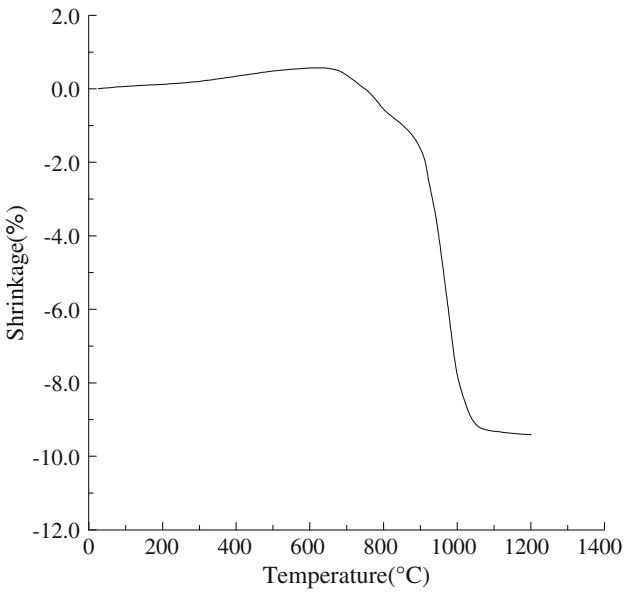

Fig. 2 Shrinkage curve of the β-TCP/BG powder compact

The densification behavior of β-TCP/BG powder compacts as a function of temperature is shown in Fig. 2. A discontinuity in shrinkage rate was observed in the curve. The shrinkage rate in the temperature of 710–780°C is slightly lower than those of 910–1,010°C. According to the DSC curve of the quenched glass powder shown in Fig. 3, two crystallization events at 712°C, 778°C and a melting event at 916°C were observed. It suggests that the low shrinkage rate in the temperature of 710–780°C may be originated from the precipitation of new phase (crystallization from glass). A high shrinkage rate was observed at the temperature of 910–1,010°C. From DSC curve, it could conclude that the high shrinkage rate might be associated

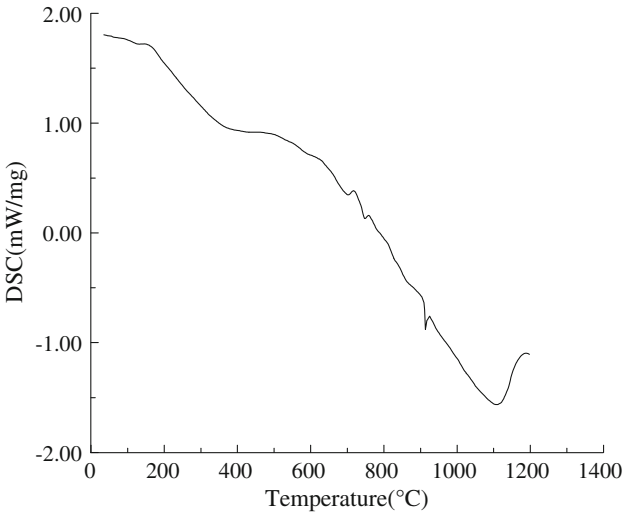

Fig. 3 Differential thermal analysis (DSC) curve for the bioglass powder

with the viscous flow of the melted liquid formed by the residual glass melting at around 920°C. Another low shrinkage rate occurred in the temperature range of 1,010–1,060°C might attributed to the reaction between β-TCP matrix and glass. The new phase formed during sintering confirmed the result. Because crystallization occurs before sintering is nearly complete, the viscosity will increase to near infinity and sintering will stop. Therefore, 1,100°C was selected as the final sintering temperature. In comparison with the pure porous β-TCP ceramic fabricated by powder sintering at a high temperature of 1,250°C [26], the β-TCP containing glass in this present work can be prepared by firing at a considerably lower temperature of 1,100°C.

The method used in this study to fabricate macroporous β-TCP based ceramic scaffolds was shown to be successful in the achievement of total porosity values over the range of 70–84%. The control of the porosity in the sintered samples can be attained by changing the solid loading and the dipping degree in the processing of the slurries, which yielded the porous green samples.

Figure 4a shows a micrograph of the polyurethane networks consisting of a large number of struts. After dipping the foams into slurry of the mixture of glass and β-TCP powder and followed by sintering at 1,100°C for 4 h, the microstructure is shown in Fig. 4b–d. The macropore sizes in the samples are distributed in the range of 100–500 μm. The macropores correspond well to the shape and size of the original porous polyurethane scaffolds. Most of the micropores formed by the gelatin and polyurethane elimination during sintering interconnected with pore size

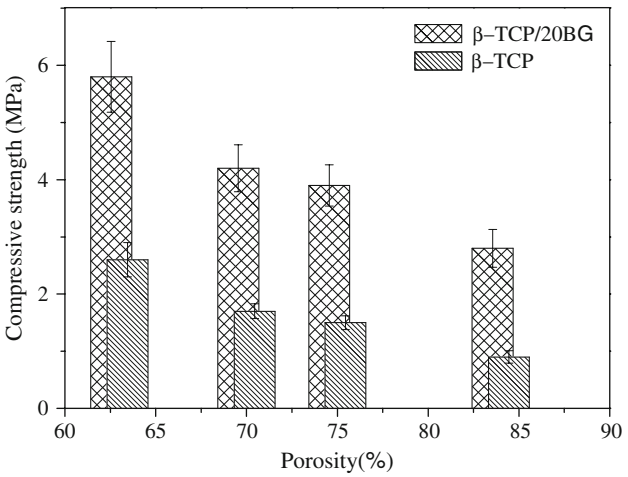

Fig. 5 Comparison of compressive strength of porous β-TCP/20BG and β-TCP scaffolds

around 5 μm. Thus, porous β-TCP/BG ceramics with both macroporosity and microporosity were obtained in this study. The comparison of the compressive strength of β-TCP/BG and pure β-TCP porous specimens is shown in Fig. 5 as a function of the porosity. The compressive strengths of all the β-TCP/BG with the similar porosity (>60%) as those of β-TCP porous specimens fabricated by the same method were significantly improved by doping 20 wt.% BG. For β-TCP/BG, the specimens with ~70% and ~84% porosity were chosen, which have an average compressive strength of 4.2 MPa and 2.8 MPa, respectively, and a good interconnect structure between the marcopores as shown in Fig. 4b and c, while the

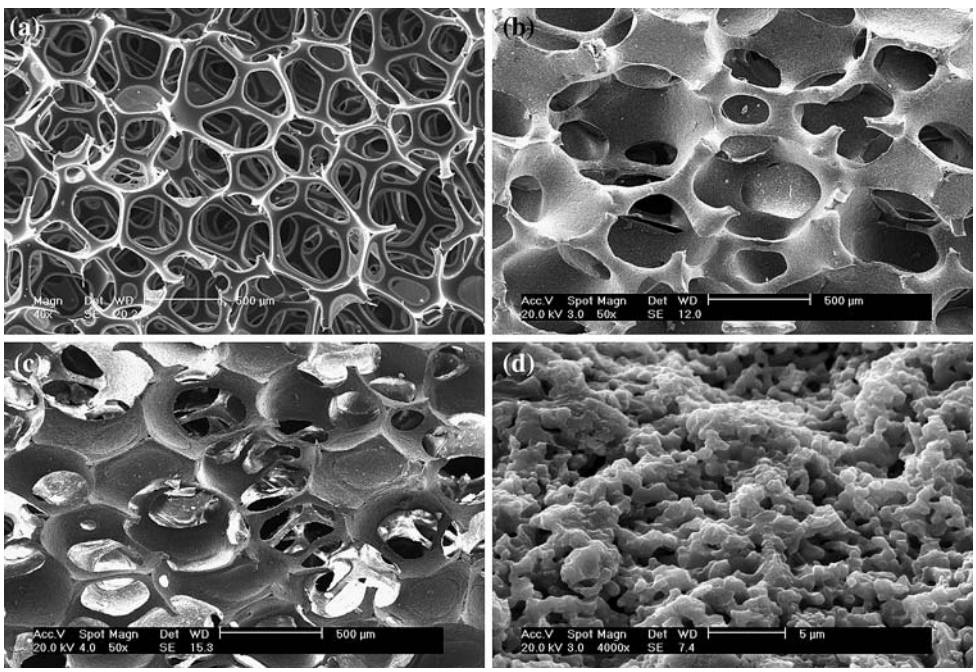

Fig. 4 SEM micrographs of the polyurethane sponge (**a**) and the sintered scaffold of β-TCP/BG with 75% porosity (**b**), 84% (**c**) and the strut (**d**), respectively

corresponding average compressive strength of β-TCP is 1.7 MPa and 0.9 MPa.

The bioglass contained in the β-TCP matrix could be considered as the "intermediate liquid phase" during sintering process. That is, the bioglass could decrease the sintering temperature to 1,060°C by the viscous flow due to the glass melting at a relative low temperature. While at a higher temperature, crystallization from glass matrix or synthesis of new phases by the reaction between β-TCP matrix and amorphous glass would improve the strength of grain boundaries.

3.2 Biological characteristics

Figure 6a shows the surface of the β-TCP/BG immersed in SBF media for 2 weeks. No continuous apatite layer was formed on the surface, but some apatite agglomerates were dispersed on the surface randomly, and the Ca/P molar ratio determined by EDS analysis is $\sim$1.42, less than the standard Ca/P ratio of 1.67 of stoichiometric hydroxyapatite (HA) and the original composition of the β-TCP/BG samples. As shown in Fig. 6b, at a magnification of $\times$10,000, it was observed that the agglomerates were composed of plate-like apatite crystallines. While no apatite layer was found on β-TCP scaffolds (Fig. 6c). The apatite formation is an in vitro bioactivity indicator of candidate hard tissues. The Ca/P molar ratio of the β-TCP/BG is less than that of β-TCP ceramic. In vitro apatite agglomerates on the surface of β-TCP/BG samples suggest that apatite formation is mainly a chemical composition dependent.

Dissolution studies were also performed to determine the solubility of porous β-TCP/BG and β-TCP in a distilled water environment and then to assess its influence to a physiological environment. The dissolution of the ions from samples in distilled water as shown in Fig. 7 confirmed that the chemical durability of porous β-TCP/BG constituted by residual amorphous glass and crystallization phases which contain sodium and magnesium ions such as $NaCaPO_4$, is lower than that of associated porous β-TCP

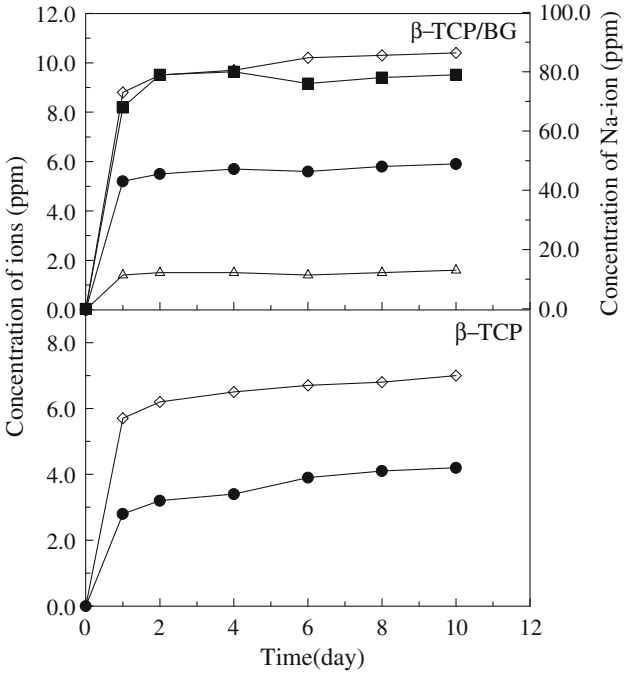

Fig. 7 Ion concentrations from β-TCP/BG and β-TCP dissolved in distilled water for different time ●: Ca^{2+},◇: P^{5+}, ■: Na^{+}, △: Mg^{2+}

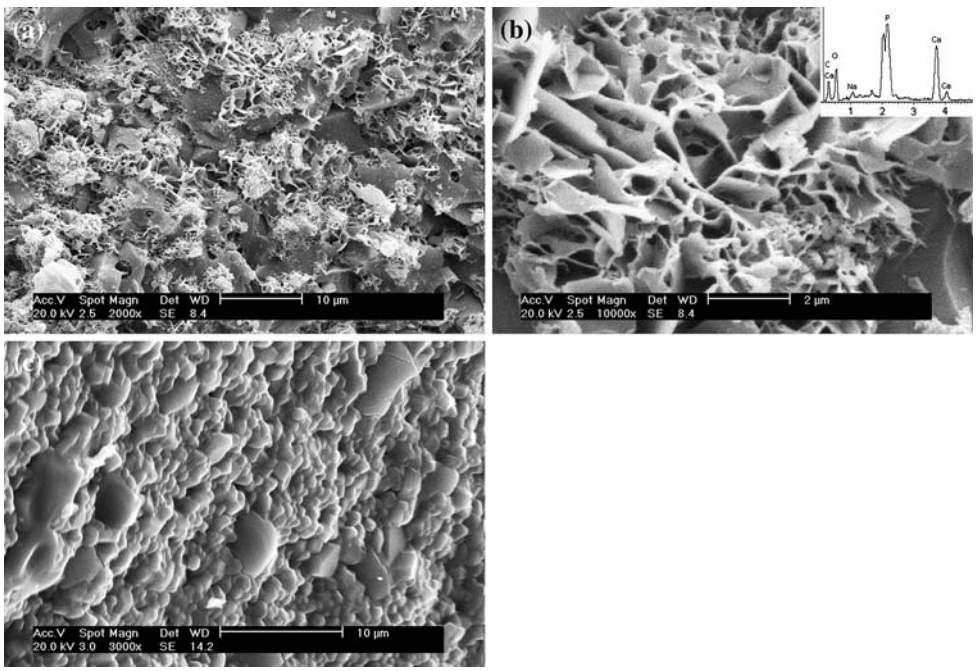

Fig. 6 SEM micrographs of β-TCP/BG (**a**, **b**) and β-TCP (**c**) ceramic surfaces after 2 weeks of immersion in culture media

ceramic. The concentrations of Ca^{2+} and P^{5+} ions released from β-TCP/BG and β-TCP were very small and were determined to be less 10 ppm. However, from β-TCP/BG samples, the dissolution of Na^{+} ions was much higher as compared to those of Ca^{2+} and P^{5+} ions, reaching to 80 ppm. The Mg^{2+} ion level was less 2 ppm, implying that the durability of the crystallized phases containing sodium ions is lower than that of crystallized phase containing magnesium ions. Meanwhile, the pH of the solution containing β-TCP/BG scaffolds changed from the original distilled water 6.9–7.2 after 4 day immersion, while the solution of β-TCP is 7.0. In fact, the pH around the scaffold should be higher than 7.2. The dissolution of Na^{+} and Ca^{2+} ions from the surface of β-TCP/BG samples would lead to locally increase of the pH value of the surrounding fluid that has a strong effect on the relative solubility of different phosphate phase, resulting in precipitation of new apatite crystals on the surface of the β-TCP/BG, which then changes the supersaturation of the surround solution. The Na^{+} ion incorporation into the apatite crystals was confirmed by EDS analysis. However, no Mg^{2+} ion was detected in the apatite crystals. Mg^{2+} ions existing in glass are known to suppress apatite crystallization in some conditions [27], and this fact might be the primary reason why no continuous apatite layer was formed on the surface when porous β-TCP/BG scaffolds were directly immersed in SBF liquid. It implies that the high pH value of the solution containing the β-TCP/BG scaffolds, resulting from

Table 1 The number of MC3T3-E1 cells were eluted under culture during 2 days,4 days and 6 days ($\times 10^5$)

Samples	2d		4d		6d	
	β-TCP/BG	β-TCP	β-TCP/BG	β-TCP	β-TCP/BG	β-TCP
1	2.91	1.52	4.09	2.73	4.96	3.62
2	3.08	1.42	4.36	2.81	5.12	3.82
3	2.72	1.39	4.12	2.66	5.21	3.69
4	2.84	1.62	4.26	2.53	4.92	3.95
5	3.02	1.47	4.14	2.76	4.93	4.02
6	2.91	1.42	4.01	2.72	5.13	3.81
7	2.79	1.51	4.12	2.51	5.21	3.90
8	3.02	1.43	4.14	2.69	4.92	4.02
X ± s	2.913 ± 0.12	1.47 ± 0.075	4.15 ± 0.11	2.68 ± 0.11	5.05 ± 0.13	3.85 ± 0.15

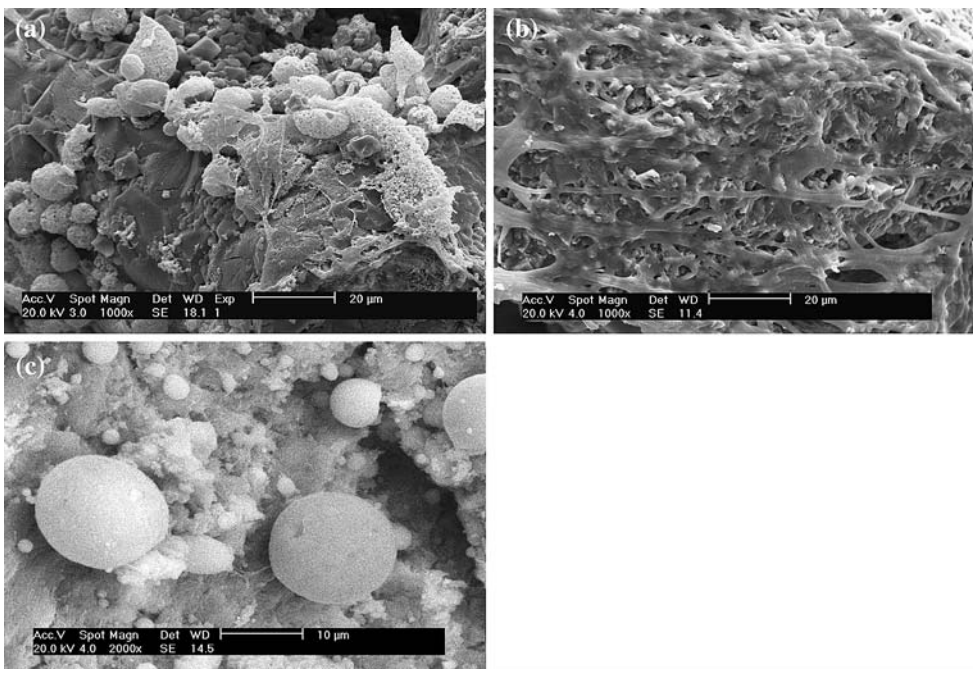

Fig. 8 SEM micrographs of osteoblasts after 2 week culture on β-TCP/BG (**a**, **b**) and β-TCP (**c**) scaffolds

the release of inorganic ions from the crystallization phases and residual glass, has profound effects on the formation of apatite layer.

To test cytotoxicity and biological characteristics, β-TCP/BG and β-TCP samples were cultured with MC3T3-E1 cells for different days, and the eluted cells were used to enumerate number of living MC3T3-E1 cells of the matrices. The statistics analysis in Table 1 shows the comparative number of cells in two kinds of scaffolds after being cultured for different time. These combined results indicate that the porous β-TCP/BG scaffolds are better than that of the porous β-TCP scaffolds on supporting the adhesion, proliferation of the MC3T3-E1 cells. In order to directly observe the interaction between materials and cells, scanning electron microscopy was carried out on the 2 week culture samples. Figure 8a is a SEM of the surface of β-TCP/BG with 75% porosity, revealing that osteoblasts attached and almost completely spread on the sample forming a continuous layer in which single cells were observed accidentally. From the cross section of porous samples, the uniform formation of extracellular matrix was observed (Fig. 8b). On the contrary, no continuous layer was evident on the pure β-TCP scaffolds (Fig. 8c). This SEM information confirms the results of Xin RL. et al's report [28] that one of the main regulators of cell adhesion in anchorage is the chemical composition of the materials, which can influence the microenvironment of the cell activity.

4 Conclusion

The objective of this study is to improve the compressive strength and osteoblasts function of β-TCP ceramics by introducing calcium phosphate based glass and optimizing the processes of the sintering process.

In the present study, calcium phosphate based glass was introduced to the β-TCP matrix as an intermediate liquid that acts as a sintering aid at a relatively low temperature during sintering. While sintered and heat-treated at the crystalline temperatures, Crystallization from amorphous glass in the β-TCP matrix was observed. The crystallization and the residual glass could not only improve the compressive strength but also adjust the release degree of inorganic ions that would influence the bioactivity of the β-TCP/BG scaffolds.

Acknowledgements Authors are grateful to financial support of China Natural Science Foundation (Grant No. 50772072), Tianjin Natural Science Foundation (Grant No. 06YFJMJC02900) and Shanghai Science Foundation (Grant No. 07QA14069).

References

1. R. Langer, J.P. Vacanti, Science **260**, 920 (1993). doi:10.1126/science.8493529
2. D.W. Hutmacher, Biomaterials **21**, 2529 (2000)
3. A.R. Boccaccini, V. Maquet, Compos. Sci. Technol. **63**, 2417 (2003). doi:10.1016/S0266-3538(03)00275-6
4. D.C. Tancred, A.J. Carr, B.A.O. Mccormack, J. Mater. Sci. Mater. Med. **12**, 81 (2001). doi:10.1023/A:1026773522934
5. V.V. Silva, F.S. Lameiras, R.Z. Domingues, Compos. Sci. Technol. **61**, 301 (2001). doi:10.1016/S0266-3538(00)00222-0
6. W. Suchanel, M. Yashima, M. Kakihana, M. Yoshimura, Biomaterials **17**, 1715 (1996). doi:10.1016/0142-9612(96)87652-6
7. Y.K. Juna, H.K. Wan, O.K. Kweonb, S.H. Honga, Biomaterials **24**, 3731 (2003). doi:10.1016/S0142-9612(03)00248-5
8. V. Salih, A. Patel, J.C. Knowles, Biomed. Mater. **2**, 11 (2007). doi:10.1088/1748-6041/2/1/003
9. T. Kokubo, H.M. Kim, M. Kawashita, Biomaterials **24**, 2161 (2003). doi:10.1016/S0142-9612(03)00044-9
10. R. Murugan, S. Ramakrishna, Mater. Lett. **58**, 230 (2003). doi:10.1016/S0167-577X(03)00451-8
11. T. Matsuno, M. Morita, K. Watanabe, K. Ono, M. Koishi, J. Mater. Sci. Mater. Med. **14**, 247 (2003). doi:10.1023/A:1023464115384
12. Towler, I.R. Gibson, S.M. Best, J. Mater. Sci. Lett. **19**, 2209 (2000). doi:10.1023/A:1006752202731
13. V. Salin, G. Georgiou, J.C. Knowles, I. Olsen, Biomaterials **22**, 2817 (2001). doi:10.1016/S0142-9612(01)00026-6
14. S. Langstaff, M. Sayer, T.J.N. Smith, S.M. Pugh, Biomaterials **22**, 135 (2001). doi:10.1016/S0142-9612(00)00139-3
15. G. Goller, H. Demirkiran, F.N. Oktar, E. Demirkesen, Ceram. Int. **29**, 72 (2003)
16. O. Peital, E.D. Zanotto, L.L. Hench, J. Non-Cryst. Solids **292**, 11 (2001)
17. M. Nagase, Y. Abe, M. Chigira, E. Udagawa, Biomaterials **13**, 172 (1992)
18. M.H. Prado Da Silva, A.F. Lemos, I.R. Gibson, J.M.F. Ferreira, J. Non-Cryst. Solids **304**, 286 (2002). doi:10.1016/S0022-3093(02)01036-0
19. T. Kasuga, M. Sawada, M. Nogami, Y. Abe, Biomaterials **20**, 1415 (1999). doi:10.1016/S0142-9612(99)00047-2
20. H.P. Yuan, J.D. De Bruijn, Y.B. Li, J. Qfeng, Z.J. Yang, K. De Groot et al., J. Mater. Sci. Mater. Med. **12**, 7 (2001). doi:10.1023/A:1026792615665
21. K. Franks, I. Abrahams, G. Georgiou, J.C. Knowles, Biomaterials **22**, 497 (2001). doi:10.1016/S0142-9612(00)00207-6
22. S.H. Rehee, Biomaterials **23**, 1147 (2002). doi:10.1016/S0142-9612(01)00229-0
23. E. Esposoto, R. Cortesi, C. Nastruzzi, Biomaterials **20**, 2009 (1995)
24. Y. Otani, Y. Tabata, Y. Ikada, Biomaterials **19**, 2091 (1998). doi:10.1016/S0142-9612(98)00121-5
25. J. Ando, S. Matsuno, Bull. Chem. Soc. Jpn. **41**, 342 (1968). doi:10.1246/bcsj.41.342
26. M. Jarco, R.L. Salabury, M.B. Thomas, R.H. Diremus, J. Mater. Sci. **14**, 142 (1979). doi:10.1007/BF01028337
27. N.C. Blumenthal, Clin. Orthop. Relat. Res. **248**, 279 (1989)
28. R.L. Xin, Y. Leng, J.Y. Chen, Q.Y. Zhang, Biomaterials **26**, 6477 (2005). doi:10.1016/j.biomaterials.2005.04.028